Polyboride Networks, Molybdenum Clusters, and Uranium Bonding

Erika F. Merschrod S. and Roald Hoffmann*

Department of Chemistry and Chemical Biology and Cornell Center for Materials Research, Cornell University, Ithaca, New York, 14853-1301

The extended Hückel tight-binding method is used to analyze the bonding in the boron, molybdenum, and uranium substructures as well as the B−Mo interactions in $U_5Mo_{10}B_{24}$. This compound, recently synthesized by Jeitschko and co-workers, contains relatively close U−U contacts, molybdenum clusters, and several different one- and two-dimensional polyboride structures. Molecular orbital calculations support a formal electron partitioning as follows: B_{14}^{16-} for a one-dimensional graphitic strip kinked at an "inserted" boron; B_{10}^{12-} for a simpler graphitic strip; B_7^{10-} for an unusual propellane-like one-dimensional polymer. The tetrahedral Mo clusters and U needles are also examined in analyzing the electronic structure of this unique compound sublattice by sublattice. With respect to the formation of this compound vs the originally expected $U_5Mo_{10}B_{30}$ (presumably analogous to $ThCr_2B_6$), the results indicate that the higher metal:boron ratio creates more opportunity for metal−metal and metal−boron contact, leading to more Mo−Mo bonding than that found in the hypothetical $U_5Mo_{10}B_{30}$.

Introduction

Binary and ternary borides display a rich structural chemistry, with boride substructures ranging from zero-dimensional units isolated from each other in a matrix of metal atoms to two- and three-dimensional networks of 3-, 4-, 5-, and higher-membered rings.[1,2] A compound synthesized recently by Jeitschko and co-workers contains no less than three different one- and two-dimensional polyboride substructures.[3] This novel compound, $U_5Mo_{10}B_{24}$, also displays interesting Mo−Mo bonding in chains of vertex-sharing tetrahedral clusters. The variety of these structures caught our interest in the context of developing an understanding of nonclassical electron-deficient and electron-rich three-center bonding in extended structures.

The $U_5Mo_{10}B_{24}$ Structure

Structure **1** shows one view of $U_5Mo_{10}B_{24}$ as observed along the *a*-axis. (The crystallographic directions *a*, *b*, and *c* correspond to the Cartesian directions *x*, *y*, and *z* in the illustrations.) At the left the elaborate connectivity of the three polyboride sublattices is highlighted; each boride sublattice is connected by dark lines. At the right, we indicate the molybdenum clusters, also with dark lines.

There are short uranium−uranium contacts of 3.1 Å forming one-dimensional needles which run along the *a*-axis. These distances are similar to those in elemental U (bcc), and indicate some bonding interaction between the uraniums. There are also short U−Mo contacts,

1
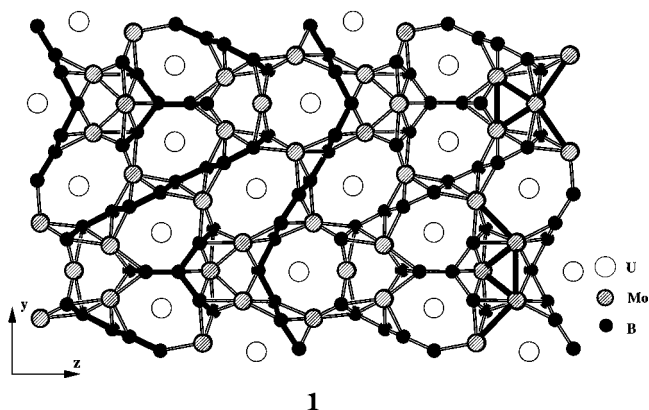
which suggest some electronic interaction between those atoms. We are reluctant to call the latter interactions "bonds" because, as will become apparent when we discuss Mo coordination, the Mo in question [Mo(5)] is already highly coordinated by other Mo's and by boron. These U−Mo interactions are bonding, though, as will be seen later. The U−U interactions, however, seem quite strong and will be explored.

How shall one partition the electrons in this ternary boride? A Zintl−Klemm approach might begin with a 6+ oxidation state for U. However, the short U−U contacts suggest that these atoms have some electrons associated with them. The other common choice for U would be +4. Thus as a starting point we could have $U_5^{20+}(Mo_{10}B_{24})^{20-}$ or $U_5^{30+}(Mo_{10}B_{24})^{30-}$. The electronegativities for U, Mo, and B are 1.7, 1.8, and 2.0,[4] respectively, so we are driven toward more positively charged

(1) Etourneu, J. *J. Less Common Metals* **1985,** *110,* 267.
(2) Rogl, P. *J. Less Common Metals* **1985,** *110,* 283.
(3) Konrad, T.; Jeitschko, W. *J. Alloys Compd.* **1996,** *233,* L3.

(4) Pauling, L. *The Nature of the Chemical Bond*, 3rd ed.; Cornell University: Ithaca, NY, 1960.

U's and more negatively charged B's, with the Mo's compensating for the difference. Our "electron counting" is based on these electronegativities.

At this point it is important to mention that when $U_5Mo_{10}B_{24}$ was first synthesized, it was tentatively assigned the stoichiometry UMo_2B_6.[5] An analogous compound does exist, $ThCr_2B_6$,[6] which has the $CeCr_2B_6$ structure type.[6,7] The electron counting in the thorium compound is straightforward. The borons are linked into a three-connected network, which leads to a 1− charge if one completes the octet around each B (assuming trigonal borons). Thorium rarely occurs in an oxidation state other than 4+.[8] There are short Th−Th contacts in $ThCr_2B_6$, but the Th's have many more B contacts than the U's in $U_5Mo_{10}B_{24}$ (16 vs 10−14), so one would expect that these close Th−Th contacts are due more to interactions with the polyboride and less to rare-earth bonding than in $U_5Mo_{10}B_{24}$. This leaves Cr_2^{2+} which forms dimers (Cr−Cr 2.58 Å) coordinated by 16 borons, four of which are bridging the Cr−Cr bond. Because each B is a one-electron donor (through the π system), each chromium has 14 electrons around it. Six electrons come from the six "terminal" borons, two come from the four bridging borons, one comes from the other Cr, and five come from the Cr^+ itself.

In the next few sections we will compare the electronic structure of the transition metal and boron sublattices in $U_5Mo_{10}B_{24}$ and $ThCr_2B_6$ (as a model for the hypothetical UMo_2B_6). In the process we will explore the possible reasons why $U_5Mo_{10}B_{24}$ was formed, instead of $U_5Mo_{10}B_{30}$.

The Boride Substructures

Three different polyboride substructures are found in the crystal structure of $U_5Mo_{10}B_{24}$. First, there are one-dimensional strips of graphitic nets, which are six borons wide and whose edges are joined at angles by a seventh set of borons to form kinked sheets. These sheets (**2**) are made up of six-membered planar rings and eight-membered bent rings. Looking along the *a*-axis (see **2**), one sees these zigzag sheets edge-on, propagating in the *b* direction. These sheets are spaced about every 15 Å along the *c* direction.

2
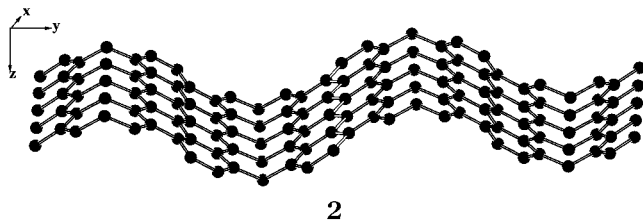
The second substructure one finds is also derived from graphite-like sheets. One-dimensional strips of B hexagons propagate along the *a* direction and are 10 borons wide (**3**). These strips are canted relative to each other, forming a zigzag array along the *b* direction. However,

the edges of the strips are 3.5 Å apart, unlike the sheets mentioned previously in which strips are joined in the second dimension by additional B links.

3
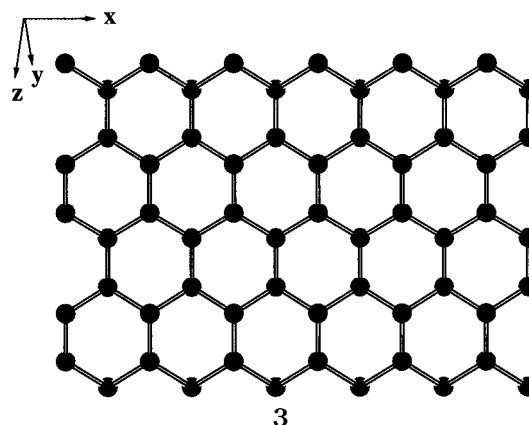
The third substructure repeats the bent, eight-membered ring motif of the first, but has an additional B link across the ring, forming a propellane-like geometry. This is repeated to form a one-dimensional chain in the *a* direction, as shown in **4**. An alternative description of this fascinating one-dimensional structure is that it consists of three polyacetylene-like B chains linked to a line of centering borons. This one-dimensional topology is also found in $Ba_2Eu_3Si_7$[9] (where, we will see, it has a different electron count) and has been investigated as a possible conducting hydrocarbon[10] and as a $Cu(N_2)_3$ chain.[11] To show the stoichiometric relationship of the various substructures, we double the formula unit to B_{48}. One then has $^2_\infty[B_{14}]\,^1_\infty[B_{10}]_2\,^1_\infty[B_7]_2$.

4
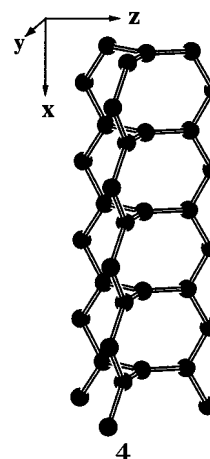
The ThCr₂B₆ Structure

For comparison we show the crystal structure of $ThCr_2B_6$ in **5**. The motifs in the boride substructures of $ThCr_2B_6$ are similar to those in $U_5Mo_{10}B_{24}$, but will not be illustrated in such detail. In $ThCr_2B_6$ there are needles of three-connected borons linking two polyacetylenic chains (instead of three as in **4**), and kinked sheets of bent eight-membered rings (like abbreviated versions of **2**). However, these individual boride motifs are linked

(5) Val'ovka, I.; Kuz'ma, Y. *Sov. Powder Metall. Met. Ceram.* **1986**, *25*, 986.

(6) Konrad, T.; Jeitschko, W.; Danebrock, M. E.; Evers, C. B. *J. Alloys Compd.* **1996**, *234*, 56.

(7) Kuz'ma, Y. *Sov. Phys. Crystallogr.* **1970**, *15*, 312.

(8) A lone example of Th³⁺ is described by A. M. Koulkes-Pujo et al. *Nouv. J. Chim.* **1982**, *6*, 571.

(9) Häussermann, C.; Nesper, R. *Angew. Chem., Int. Ed. Engl.* **1995**, *34*, 1462.

(10) Hoffmann, R.; Eisenstein, O.; Balaban, A. T. *Proc. Natl. Acad. Sci. U.S.A.* **1980**, *77*, 5588.

(11) Merz, K. M., Jr.; Hoffmann, R. *Inorg. Chem.* **1988**, *27*, 2120.

to form a three-dimensional net. There are also similarities in the arrangements of the transition metal and rare earth atoms. In $ThCr_2B_6$, the thorium lies between two bent eight-membered B rings; in $U_5Mo_{10}B_{24}$, two of the three crystallographically unique uraniums are coordinated by similar rings (from **2** or **4**; see Scheme 1). The Cr atoms in $ThCr_2B_6$ are found in pairs straddling a bent 8-ring; four of the six Mo atoms in $U_5Mo_{10}B_{24}$ are also found in pairs, and some of those straddle bent 8-rings as well.

5
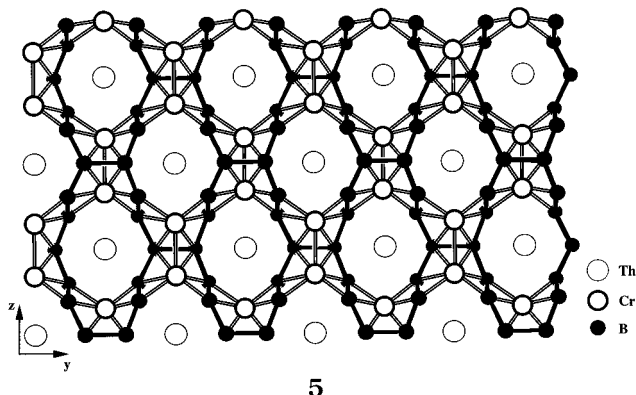
There are clearly differences in these two structures as well. The fantastic complexity in $U_5Mo_{10}B_{24}$ follows from the many different types of boron coordination found. This different connectivity in the polyborides gives rise to electron counts different than that for the B network in $ThCr_2B_6$, as we will see shortly. In addition, there is much more Mo–Mo bonding in $U_5Mo_{10}B_{24}$ than Cr–Cr bonding in $ThCr_2B_6$.

There are many other examples of borides with benzenoid ring substructures; these have been discussed extensively elsewhere.[12–14]

Sheets and Ribbons

Returning to the ternary U phase, one can easily arrive at a reasonable electron count for the first substructure, the kinked sheets (**2**), by exploiting its structural similarities to graphite. From the trigonal planar coordination around the borons, one can expect the three-connected borons (members of 6-rings) to have available a 2p orbital perpendicular to the local plane. The octet is complete with one double bond and two single bonds, requiring four electrons per boron and thus a 1– charge per three-connected atom. The 2-connected (bridging) boron has two electrons in σ bonds and one in a π bond. It needs two more electrons to complete the octet (formally a lone pair pointing along the *c* direction), yielding a 2– charge. To the 14 borons in the unit cell we thus assign (in a preliminary way, we are just formulating a possibility) a formal charge of 16–. This is certainly rather high! However, if we were to fill every nonbonding orbital on B with electrons (thus negating all π bonding) we would be led to an even more unrealistic B_{14}^{30-}. Let's keep in mind that this is only a

formalism, and that electrons are probably shared with the Mo atoms that are in close contact with these kinked sheets.

The electrons in the one-dimensional graphitic ribbons **3** are assigned in a similar fashion. The inner B's, being three-coordinate, are assigned a 1– charge (one electron in the π system). The two-coordinate edge B's each have two electrons in σ bonds, one electron in the π system, and two electrons in a "lone pair" to complete the octet, so they are each formally 2–. This gives a 12– charge per B_{10} unit cell.

The Propellane Column

The last substructure can be viewed as three polyacetylene-like chains linked by a collinear column of tricoordinate borons, or as a column of fused propellane-like moieties. Continuing with the analogy to carbon, we consider the borons on the inner edge of the chains (bound to the central B) as locally trigonal, so they can be counted as 1–. The outer boron atoms of the chains are two-coordinate, so they carry a 2– charge (a lone pair pointing away from the center of the column). The central B is three-coordinate; assuming little possibility for π-type interactions with the outer chains (because of the orientation of its p orbital perpendicular to the π system of those chains), it requires an additional two electrons to complete the octet. We therefore tentatively assign to the central B a lone pair of electrons along with its three σ bonds, giving a formal 2– charge on that boron and a total formal charge for the substructure of $^1_\infty[B_7^{11-}]$.

There are some silicon structural analogues to this polyboride which provide an alternative electron-counting scheme devoid of π bonding.[9,15] Might these polyborides be isoelectronic to, for example, the $^1_\infty[Si_7^{10-}]$ chains in $Ba_2Eu_3Si_7$? The correspondingly charged boride chain, $^1_\infty[B_7^{17-}]$, would preclude the possibility of any π bonding between borons. This is inconsistent with the B–B bond lengths in the polyacetylenic chains (1.79 Å in one chain, 1.85 Å in the others). These bond lengths are similar to those found in the graphitic sheets, where they were involved in a trigonal planar network and thus were assigned a bond order of 1.5, which assumes some delocalization of the π system. In addition, a charge of 17– on seven borons is very high! For these two reasons this silicide may not be a good electronic model for **4**, although its structure is very similar to the one we are examining.

Another structure, similar to these polyboride columns but made of carbon, is found in the [3,3,3]propellanes.[16] Similar molecules also have been synthesized with N, Si (the so-called "silatranes"), and/or B replacing one or both bridgehead carbons. This class of molecules presents another perspective on the bonding in **4**. Propellanes have a bond between the bridgehead atoms, but there have been theoretical explorations into creating the corresponding diradical species (dissolving the bridging bond), mostly through the effects of steric strain.[10,17] If we were to use

(12) Matkovitch, V. I., Ed. *Boron and Refractory Borides;* Springer-Verlag: Berlin, 1977.
(13) Minyaev, R. M.; Hoffmann, R. *Chem. Mater.* **1991**, *3*, 547.
(14) Klesnar, H.; Aselage, T.; Morosin, B.; Kwei, G.; Lawson, A. *J. Alloys Compd.* **1996**, *241*, 180.

(15) Currao, A.; Wengert, S.; Nesper, R.; Curdin, J.; Hillebrecht, H. *Z. Anorg. Allg. Chem.* **1996**, *622*, 501.
(16) Ginsburg, D. *Propellanes: Structure and Reactions;* Verlag Chemie: Weinheim, 1975.
(17) Stohrer, W.-D.; Hoffmann, R. *J. Am. Chem. Soc.* **1972**, *94*, 779.
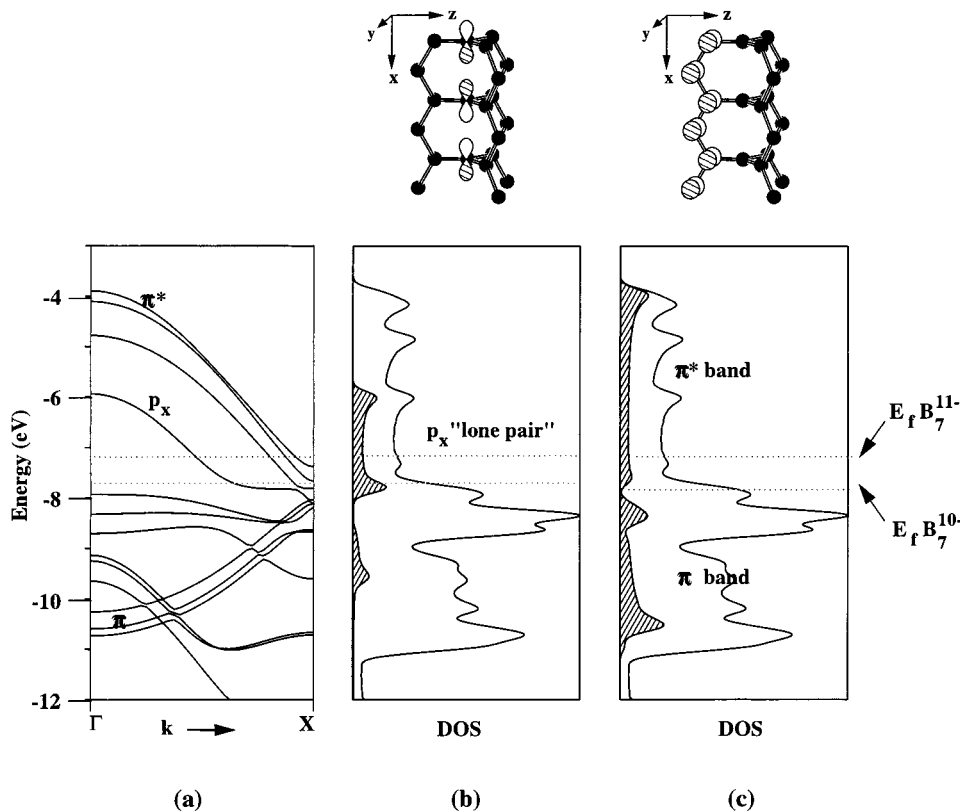
Figure 1. (a) Band structure near the Fermi level of **4**, with side-chain π bands marked. Contributions to the DOS of **4** near the Fermi level by the p_x orbitals on the central B atoms (b) and by the π and π^* bands of one polyacetylenic side chain (c). The upper Fermi level is for the central B with a lone pair; the lower one is for the central B as a radical.

propellanes as a basis for electron counting in **4**, we would begin assigning formal charges as we did originally, with 2− on the outer-edge atoms and 1− on the inner-edge atoms. At this point we are faced with a dilemma about how many electrons to put on the central boron atoms. In propellanes, the bridgehead atoms are either bound to each other or they are radicals, and in either case they have formally 4 electrons each. This would give us a 1− charge on the central B (instead of the 2− we assigned formerly) and thus a 10− charge for this structure. This contribution (doubled, for the doubled unit cell), along with the 16− charge on **2** and the 12− charge on **3** (also doubled), would yield B_{48}^{60-}, matching the positive charge from ten 6+ uraniums in the unit cell.

Would this polyboride prefer the 10− charge instead of an 11− charge which satisfies (formally) the octet around the central B? One way in which the "radical" central B could be stabilized would be through bonding with other atoms. In particular, there might be some σ bonding between the central borons. We cannot go further with general considerations, and need at this point to turn to electronic structure calculations. These were performed on the isolated polymer with the crystallographic coordinates found experimentally (i.e., a distorted, not trigonal, chain).

It turns out that the bonding between the central borons is small, because they are 3.1 Å apart. But the σ (p_x) band is not completely flat; it has about 1 eV bandwidth, and is approximately half-filled for both $^1_\infty[B_7^{10-}]$ and $^1_\infty[B_7^{11-}]$. Based on that information alone, one would expect a Peierls-type (pairing) distortion in the central column, as shown in **6**. However, this p_x band

is not the only band at the Fermi level, as can been seen in Figure 1. Each "polyacetylene" B chain generates a π band; three such bands in toto. In the doubled unit cell these are "folded-back." The π bands of the polyacetylenic chains are also crossing the Fermi level, but these are more than half filled. These bands would also be changed by the hypothetical pairing distortion, leading to a lowering in energy of the lower, filled π states and a raising in energy of the partially filled π^* bands. Our calculations show a 40% occupancy of the "polyacetylene" π^* states for the undistorted (experimentally observed) geometry, with a slight increase upon distortion.
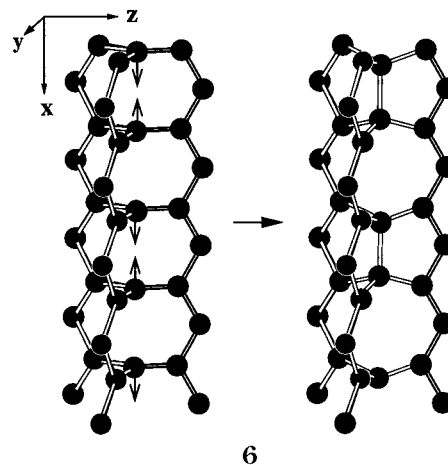
6

We think there would be a net destabilization from the pairing distortion, despite the additional bonding
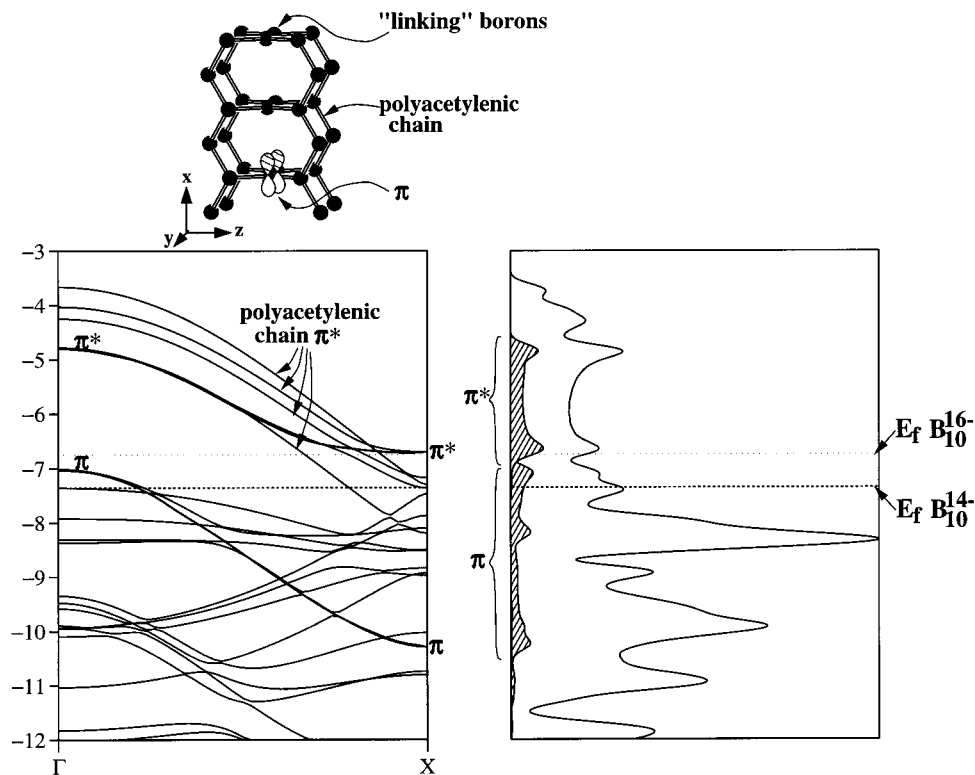
Figure 2. Band structure (left) and DOS for linking unit **8**, B_{10}^{14-}. The Fermi level is marked by the lower, heavy, horizontal dotted line. The lighter dotted line above shows the Fermi level for B_{10}^{16-}, the appropriate charge for a formal "lone pair" on each of the two linking B's. The bands with predominant π and π^* character from the linking B—B bond (p_x orbitals on the linking atoms) are marked with a heavy line, showing the dispersion across the zone if we were to neglect the mixing of these bands with others. At right we show the contributions (shaded regions) to the DOS of the linking B_2's π and π^* orbitals.

developed and the more tetrahedral coordination geometry for the central B's. No distortion is observed in the experimentally determined structure. In sum, from our calculations we find that the 11− charge does not fill a "lone pair" on the central boron but instead destabilizes the polyacetylenic side chains. The stability of these side chains also precludes a Peierls instability in the central B column. Both of these points support a 10− charge for **4**.

There is an additional feature of this polyboride which we have not yet explored. The central B is closer to one zigzag chain than to the other two (1.76 Å vs 1.90 Å). The placement of the U and Mo atoms about **4** underlines (and underlies) this asymmetry. Calculations building up the $\frac{1}{\infty}[B_{10}]$ chain from inner and outer chain sublattices indicate stronger σ bonding between the closer borons as would be expected from the shorter distance.

The Boride Sublattice in ThCr₂B₆

The polyboride sublattice in $ThCr_2B_6$ is composed of kinked sheets (similar to **2** in $U_5Mo_{10}B_{24}$) linked together into a three-dimensional network through the borons along the sheet ridges (see **7**). It is interesting to consider the linking bond between sheets, particularly in relation to the structurally similar polyboride **4**. We show in Scheme 8 two views of a one-dimensional fragment from network **7** which contains this B—B link.

As mentioned previously, each boron atom is in a planar, three-coordinate environment. If we place one electron in the p orbital perpendicular to the trigonal plane, each B can thus be assigned a formal charge of
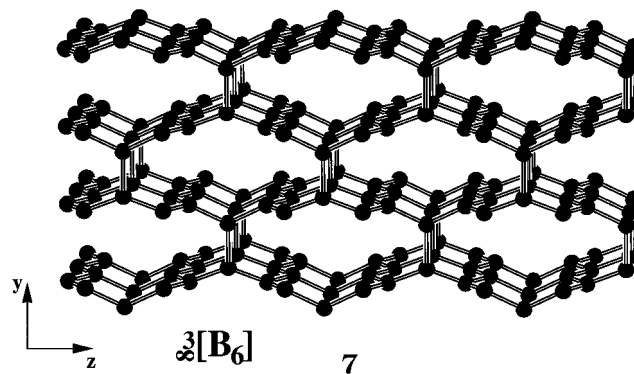
−1. In the schematic bond assignment at right in **8** we see that this choice of electron count leads to a formal double bond between the two bridging borons. (Because we are cutting this column out of a larger boron sublattice we must account for the B—B bonds broken by completing the octet for the outer B atoms with lone pairs; thus the 2− charge on the outer borons.) A projection of the contribution to the DOS curve from the π-type orbitals of these linking atoms shows that the bonding π levels are nearly filled and the antibonding π^* levels are nearly empty, indicating net strong double-bonding. (See Figure 2.) The length and overlap population of this linking bond is similar to those of the other similarly named "double" bonds in this structure and in $U_5Mo_{10}B_{24}$.

The planar, three-coordinate B in **4** and the π-bonded Bs in **8** are similar electronically, as seen in the band structures in Figures 1 and 2. As in polyboride 4 from $U_5Mo_{10}B_{24}$, additional electrons added to the unit cell

8
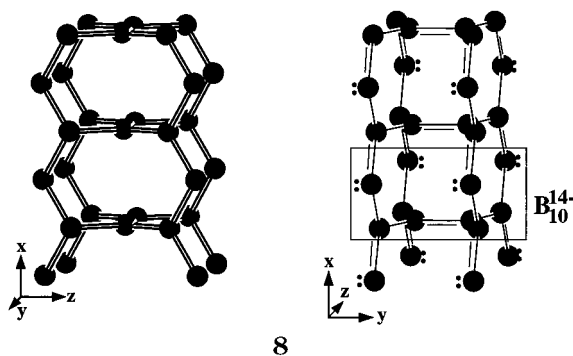
to give a formal "lone pair" on each B do not actually occupy the appropriate p_x orbitals. Instead they occupy antibonding states, between the linking borons and the outer chains and between borons in the outer chains. This additional filling of states is indicated by the upper horizontal dotted line in Figure 2.

There also appears to be significant bonding between pairs of linking borons along the chain axis (**a**) which are 3.1 Å apart. This can be seen in the large bandwidth (5 eV) of the linking π and π^* bands; this larger bandwidth corresponds to the greater interaction of these orbitals *between* unit cells. Similar systems involving interactions between stacked π systems are studied in ref 18.

In summary, we suggest that each unit in **4** carries a formal 10− (rather than 11−) charge, an electron count analogous to **7** in ThCr$_2$B$_6$. The 10− charge (along with the electron counts derived for the other boride substructures) suggests a radical trigonal planar boron within **4**. Although the 11− charge would satisfy, in a formal sense, a classical electron count (closed-shell about each boron) for **4**, our calculations indicate that rather than complete the octet around the central boron, the additional electron would fill π^* orbitals on the outer chains, hence weakening the polyboride bonding. In either case, the excess negative charge should be balanced by the molybdenum atoms. In U^{6+} we have either Mo$_{10}^0$ or Mo$_{10}^{1+}$, and for U^{4+} either Mo$_{10}^{10+}$ or Mo$_{10}^{11+}$, depending on the charge on **4**. This gives a formal charge for each molybdenum of 0, +0.1, +1, or +1.1. None of these is unreasonable. ThCr$_2$B$_6$ has a charge of +1 on the transition metal, so one might expect the same for the hypothetical UMo$_2$B$_6$ and for the structure we discuss, a variation on UMo$_2$B$_6$. In the next section we will explore these possibilities for electron count in the Mo sublattice. We will find that with the transition metal (Mo/Cr), as we have seen with B, the structural differences between ThCr$_2$B$_6$ and U$_5$Mo$_{10}$B$_{24}$ are compensated by stoichiometric differences such that these two structures are similar electronically.

Mo−B Interactions

The molybdenum clusters do not exist in isolation; the Mo−Mo bonds are supported by Mo−B interactions. At first glance the coordination polyhedra are rather complicated, and they do not seem to resemble any idealized deltahedral shape. However, if we look at the very closest contacts (Mo−B ≤ 2.3 Å) we start to see

(18) Merz, K. M., Jr.; Hoffmann, R.; Balaban, A. T. *J. Am. Chem. Soc.* **1987**, *109*, 6742.

some patterns. Ignoring the U−Mo interactions (they are mostly quite weak), let us look at the Mo−B interactions in some detail. The outermost atoms in both Mo tetrahedral chains [Mo(1) and Mo(4)] lie about 1.4 Å above the center of a B$_6$ ring from the ribbons **3** (in D$_{2d}$) or from the kinked sheets **2** (in C$_{2v}$). The Mo(4)−Mo(5) and Mo(1)−Mo(2) bonds are bridged by an additional 3 Bs.

Cluster atoms Mo(2) lie above two "B$_5$ rings" which are actually the two "facets" of the bent B$_8$ rings from boride sublattice **2**. There are similar B$_8$ rings in boride **4**, and one of those is coordinated to cluster atom Mo(6). In the C$_{2v}$ core cluster the B coordination must be different, because the Mo connectivity is different. Indeed, Mo(5) (which is highly coordinated by other molybdenums) has close contacts with B only through the aforementioned 3 borons bridging the Mo(4)−Mo(5) bonds. The Mo(3)−Mo(3) bond is bridged by three borons. In addition, each Mo(3) lies over a B$_6$ ring of **3**.

It is easier to get an overview of these complex interactions from an illustration, **9**. The $^1_\infty$[B$_{10}$] ribbon (**3**) has four rows of molybdenums over its four strips of fused B$_6$ rings, with the strips alternating between opposite sides of the ribbon. The graphitic sections of the $^2_\infty$[B$_{14}$] kinked sheet (**2**) are coordinated similarly by rows of molybdenums on alternating sides of the sheet. In addition, at the kink in the sheet there are two rows of molybdenum atoms over the two facets of the strips of fused B$_8$ rings. The $^1_\infty$[B$_7$] column (**4**) has one row of molybdenums running alongside the boron backbone, between two of the "fins".

9
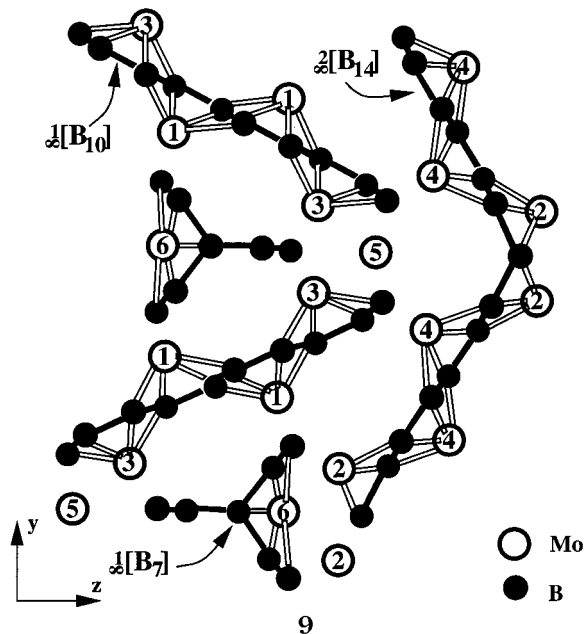
Thinking in an organometallic way, we wish to estimate the number of electrons the B network contributes to each Mo. The details of the electron counting are given in Appendix 1. We obtain in the end effective electron counts of 11 [around Mo(1) and Mo(4)], 14 [Mo-(1), Mo(3), and Mo(5)] and 17 [Mo(6)]. These are close to what we earlier found was possible for Cr in ThCr$_2$B$_6$ (14 electrons).

Hence, although it is possible for the B sublattice in ThCr$_2$B$_6$ to contribute more electrons in bonding with
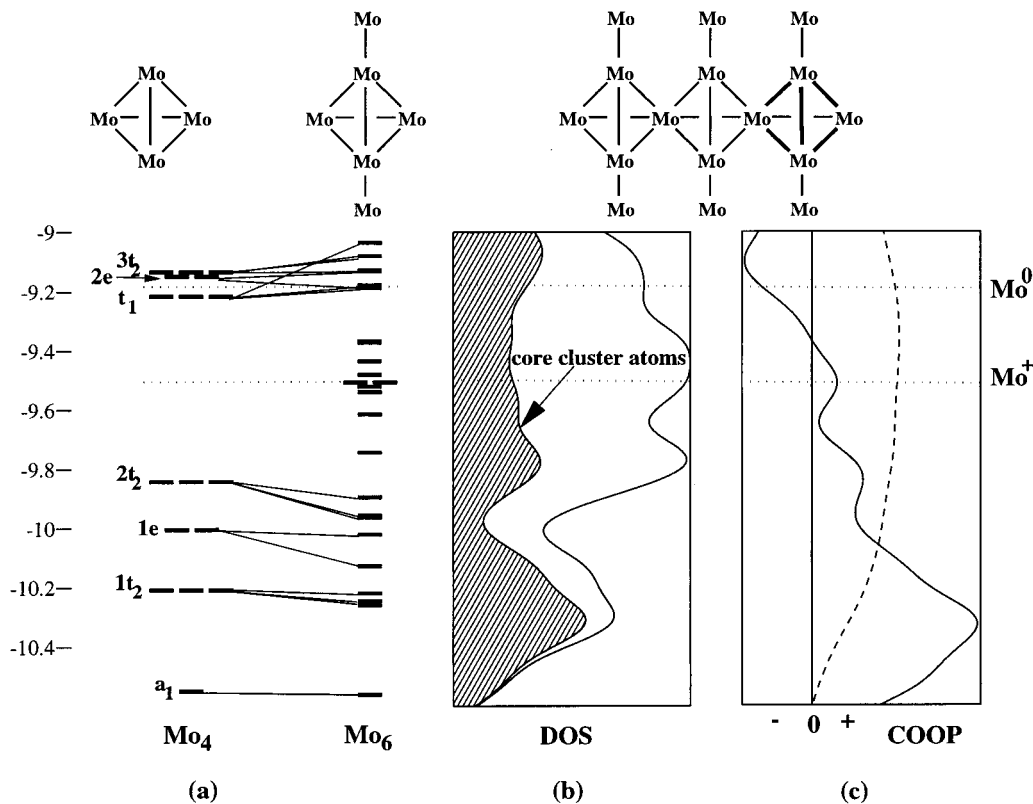
Figure 3. (a) FMO interaction diagram of T_d Mo_4 and the outer molybdenums. (b) DOS curve of $^1_\infty[Mo_5]$. The DOS contribution from the core cluster atoms is shaded. (c) COOP curve for the core cluster bonds of $^1_\infty[Mo_5]$; these bonds are indicated in bold above the plot. The dashed line is the COOP integration curve. The two Fermi levels indicated for (b) and (c) by dotted lines correspond to the different oxidation states possible for Mo depending on the oxidation state of U. These dotted lines are extended into (a) to indicate the division between filled and unfilled levels.

Cr than with Mo in $U_5Mo_{10}B_{24}$, the Mo–Mo bonding in $U_5Mo_{10}B_{24}$ more than makes up for this through many close Mo–Mo interactions not possible for Cr in the $ThCr_2B_6$ structure. Let's examine these Mo–Mo bonds.

The Molybdenum Sublattice

As discussed earlier, the 20 molybdenum atoms in the unit cell might carry a net formal charge between zero and 2+, assuming that each U carries a 6+ or a 4+ charge and depending on the electron count of polyboride chain **4**. The electron counting is a formalism, of course, and after interaction with the B sublattice there should be much charge redistribution, as we saw in the previous section. Our calculations on the $(Mo_{20}B_{48})^{60-}$ and $(Mo_{20}B_{48})^{40-}$ sublattices indicate that the negative charge is shared almost equally between Mo_{20} and B_{48}. On the other hand, a calculation including uranium[19] gives 14− on B_{48} and 3+ on Mo_{20}, with the remaining 11+ on U_{10}. In any case, for simplicity's sake, let us stick with either $(Mo_{20})^{2+/0}$ or $(Mo_{20})^{22+/20+}$, according to the extreme but clear-cut distribution of electrons outlined in the previous section for closed-shell configurations around the borons.

The Mo sublattice consists of chains of distorted, vertex-sharing Mo tetrahedra with an additional two Mo's coordinated to one or two of the vertexes of the tetrahedra. (See **10**; the core clusters of Mo are outlined with dark lines at right.) The interchain interactions

are negligible. There are two types of chains, with two of each such chains in the unit cell. One has D_{2d} distorted tetrahedra and one Mo coordinated to each unshared vertex; the other has two Mo's coordinated to each shared vertex of a C_{2v}-distorted tetrahedron.

Viewing the core clusters of these chains as distortions of tetrahedra, we can describe the bonding within them in terms of orbitals similar to those well-known radial and tangential combinations (of s and p orbitals) in *nido* trigonal bipyramidal clusters[20]: a_1 and $3t_2$ bonding and antibonding radial orbitals and $1t_2$, $1e$, and $2t_2$ bonding, nonbonding and antibonding tangential orbitals. The metal d orbitals add additional tangential molecular orbitals (MOs) of t_1 and e symmetry. Both of these are metal–metal antibonding. The energy levels for the idealized tetrahedral Mo_4 cluster are shown at left in Figure 3a.

The cluster electron count that comes from assuming Mo^0 fills the antibonding t_1 orbitals. A charge of +1.5 on each molybdenum would maximize bonding by depopulating these antibonding states. The additional two molybdenums per cluster (coordinated to the appropriate vertexes) stabilize the cluster-based bonding orbitals (those below −9.6 eV), as seen at the right in Figure 3a. The levels around −9.5 eV are based mostly on Mo(1) [or Mo(4)], and these would now be filled before the cluster-based t_1. Therefore the Mo^0 electron count would no longer be filling antibonding cluster orbitals.

---

(19) f orbitals are included in the calculation as of version 3.x, using W. V. Glassey's routine (to be published).

(20) Albright, T. A.; Burdett, J. K.; Whangbo, M.-H. *Orbital Interactions in Chemistry;* John Wiley & Sons: New York, 1985.

10
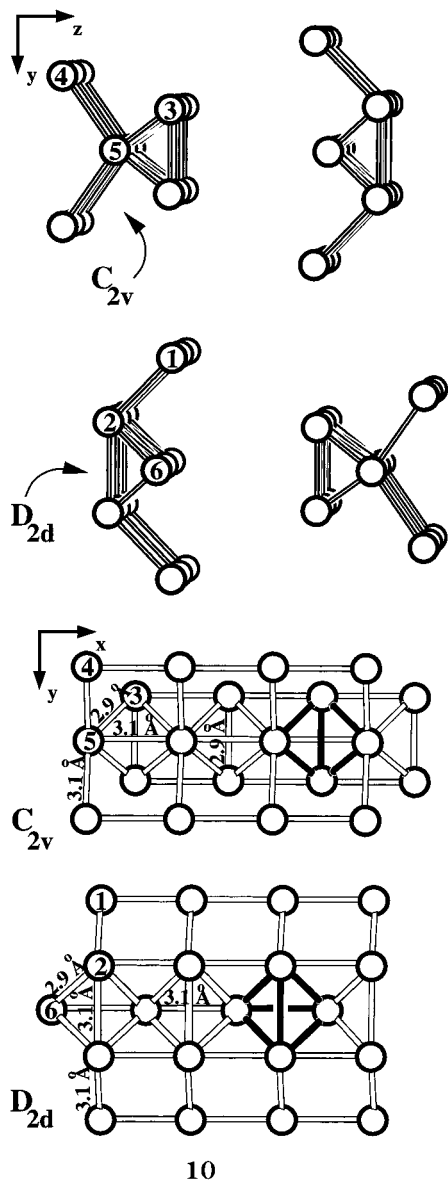
The bonding, nonbonding, and some antibonding orbitals between the core-cluster and the outer molybdenums would be occupied instead, along with the core cluster bonding orbitals. The 10 d orbitals from the outer Mo's form four bonding, two nonbonding, and four antibonding combinations with the cluster orbitals. These are the group of orbitals around −9.5 eV. The Mo's should be 1+ not to fill any of the antibonding orbitals.

We have a similar bonding picture in the extended system (chain) of tetrahedra. There are fewer atoms in the unit cell than in the isolated cluster (because of the shared vertexes) and correspondingly fewer electrons, so equivalent orbitals are filled in the chain as in the cluster. The density of states (DOS) curve of the extended system is plotted in Figure 3b; the contribution to the DOS by the core cluster atoms is indicated by the shaded region. The degree of bonding or antibonding interactions within the core cluster is reflected in the crystal orbital overlap population (COOP) curves[21] in Figure 3c. As we can see in the COOP curves, the Fermi

(21) Hoffmann, R. *Solids and Surfaces: A Chemist's View of Bonding in Extended Structures;* VCH: Weinheim, 1988.

level corresponding to Mo^{1+} (required by U^{4+}) lies just above the core cluster bonding states and just below the core antibonding states. The Fermi level corresponding to Mo^0 (following from U^{6+}) would fill core cluster antibonding states, which would not be optimal. Concerning whether the boride sublattices are 31− or 32−, the Mo sublattice does not provide a clear guide. The difference in the Fermi levels between Mo_{10}^+ and Mo_{10}^0 (or Mo_{10}^{11+} and Mo_{10}^{10+}) is about 0.01 eV, so they are essentially equal. In Figure 3b we can see that the additional positive charge on Mo_{10}^+ or Mo_{10}^{11+} would come from depopulating orbitals based mostly on Mo(4) and Mo(1).

In the D_{2d}- and C_{2v}-distorted tetrahedra, the filled orbitals are those derived for the most part from the filled orbitals of the idealized cluster. The corresponding energy bands of the chains of distorted tetrahedra are likewise similar to those of the idealized system. There are a few changes in the energy level ordering of the MOs, however, which reflect the changes in the bond lengths of the experimentally found clusters. In the D_{2d} cluster Mo(6)−Mo(6) (shared vertexes in the extended structure) and Mo(2)−Mo(2) distances are both about 3.1 Å, whereas in the C_{2v} cluster the Mo(5)'s (shared vertexes) are 3.1 Å apart and Mo(3)'s are about 2.9 Å apart (intracell). Therefore, the bonding orbitals of the bonds that are lengthened are destabilized (those derived from the a_1, $1t_2$, $1e$ and $2t_2$ in T_d), whereas the antibonding orbitals (for D_{2d}: $2b_1$ and $4e$ derived from $2e$ and $3t_2$ in T_d; for C_{2v}: $4b_2$ from $3t_2$ in T_d) are stabilized with respect to the energies in the idealized T_d cluster.

Returning to our comparison of $U_5Mo_{10}B_{24}$ with $ThCr_2B_6$, we conclude that the rare-earth and transition-metal atoms are probably in the same oxidation states formally (+4 and +1), but that the structure of $U_5Mo_{10}B_{24}$ allows for much more transition-metal bonding. The polyboride anions in $U_5Mo_{10}B_{24}$ must be more highly charged because of the higher metal:boron atom ratio, which translates into lower connectivity in the boride substructures. The higher metal:boron ratio also means more metal−metal contacts; the Mo's in $U_5Mo_{10}B_{24}$ are not separated into small boron channels such as the Cr's in $ThCr_2B_6$.

Putting It All Together: $U_5Mo_{10}B_{24}$

We have examined the interactions within each boride sublattice, within each Mo sublattice, and between select B's and Mo's. In the boride sublattices we found familiar structures, but with a twist. In strip **3** we see a carbon allotrope, but made of boron. **2** presents us with a graphitic structure, albeit one cut into segments and stitched back together into a rippled sheet. But these isolated fragments are just the starting point. The beauty of the compound is in the added complexity that creates the extravagant $U_5Mo_{10}B_{24}$ formula unit from the graphitic fragments and deltahedral clusters. Now we must examine how these substructures fit together in the complete crystal structure.

The various polyboride substructures do not interact much with each other, because they are quite far apart in the crystal lattice. Similarly, there is not much interaction between the chains of distorted Mo tetrahedra. However, we have seen that there is considerable
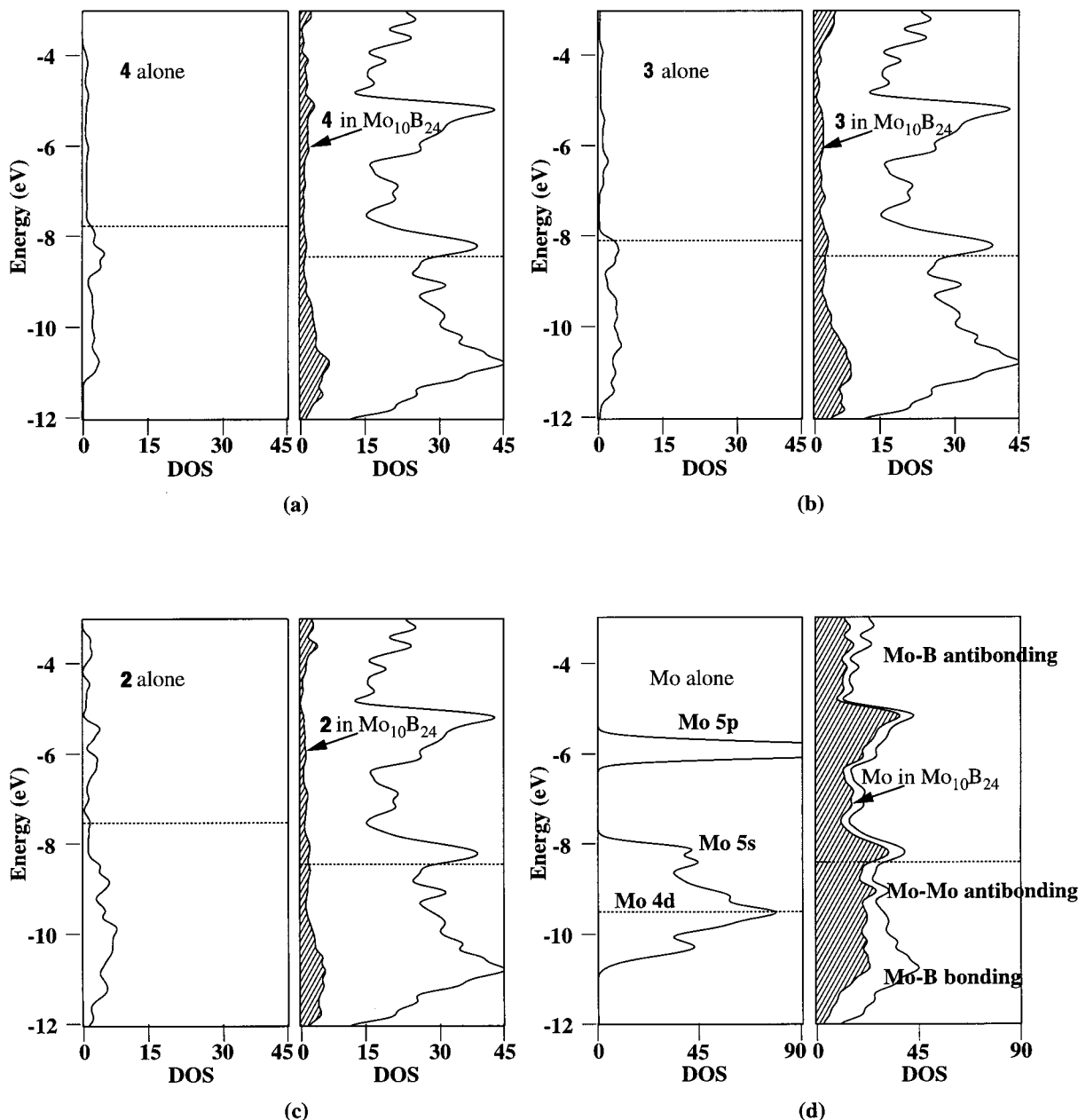
Figure 4. DOS plot of $Mo_{10}B_{24}$ compared with those of the individual Mo and B sublattices. The Fermi level of $Mo_{10}B_{24}$ corresponds to a 20− charge, which implies U^{4+}. The shaded regions at right correspond to contributions from polyborides **4** (a), **3** (b), and **2** (c), and from the Mo sublattice (d) to the DOS of $Mo_{10}B_{24}$. At left we have for comparison the DOS plots for the isolated substructures.

interaction between various Mo and B atoms. We can see how these interactions play out in Figure 4, which shows the DOS plot of the $Mo_{10}B_{24}$ sublattice with the contributions from the various B and Mo substructures. For comparison, the DOS curves of the isolated boride and Mo sublattices are also included.

The first impression is that of substantial change in the DOS of the boride sublattices upon bonding with molybdenums, which is not a surprise. The interactions between the borides and the Mo sublattice lead to B states near the Fermi level which are lowered in energy, with a corresponding lowering of the Fermi level itself. The Mo states around the Fermi level are also stabilized, but the Fermi level of $(Mo_{10}B_{24})^{20-}$ is higher than that of Mo_{10}^{10+}, corresponding to electron transfer from B_{24}^{30-}. The net charges obtained after interaction from our calculations are $Mo_{10}^{9.5-}$ and $B_{24}^{10.5-}$. The overlap populations (OPs) for the various bonds in the system

are shown in Table 1. As we can see from the overall decrease of Mo−Mo OPs, the Mo−Mo bonding is weakened. These changes in OP suggest that the charge transfer from B fills not only Mo−B bonding states but also Mo−Mo antibonding states (see Figure 3c, around −9 eV). Likewise, the B−B bonds are weakened because the bonding states of the polyborides are depopulated by the electron transfer. Of the three polyborides, **4** interacts most with the molybdenum sublattice because it has the shortest Mo−B contacts on average. (This is clear in the DOS before and after interaction; see especially the peak around −8.5 eV in the isolated sublattice. This peak is from the "lone pairs" of the outer atoms of the polyacetylenic side chains which are closest to the Mo's.) Of course, substantial Mo−B bonding is gained from the interaction. Despite this strong interaction between the outer "fins" and the Mo, the central B remains electronically similar to that in the isolated

Table 1. A Comparison of the Average OPs of Certain Mo−Mo and B−B Bonds in the Isolated Polyboride and Molybdenum Sublattices, in the $(Mo_{10}B_{24})^{20-}$ Substructure, and in $U_5Mo_{10}B_{24}$[a]

atoms	bond length (Å)	average OP		
		isolated sublattices	$(Mo_{10}B_{24})^{20-}$	$U_5Mo_{10}B_{24}$
Mo(2)−Mo(6)	2.9	0.234	0.071	0.099
Mo(3)−Mo(5)	2.9	0.185	0.051	0.080
Mo(3)−Mo(3)	2.9	0.246	0.070	0.099
Mo(2)−Mo(2)	3.1	0.088	−0.012	0.026
Mo(1)−Mo(2)	3.1	0.154	0.026	0.042
Mo(4)−Mo(5)	3.1	0.113	0.027	0.032
B−B in **2**[b]	1.8	0.973	0.752	0.628
B−B in **3**[b]	1.8	0.988	0.740	0.711
B−B in **4**[b]	1.8	0.942	0.732	0.694

[a] For calibration, the Mo−Mo OP in bulk molybdenum is 0.16 at 2.8 Å separation and 0.03 at 3.2 Å separation. [b] Average bond lengths and OPs for all of the B−B bonds in the sublattice.

column. The overall atomic charge goes down [from −0.95 in B_7^{10-} to −0.89 in B_{48}^{60-} to −0.40 in $(Mo_{10}B_{48})^{50-}$], but the orbital occupation of the p_x orbital does not change much (0.93 electrons in B_7^{10-} to 7.6 electrons in $(Mo_{10}B_{48})^{50-}$).

Up to now, we have ignored the U atoms, assuming that they are quite isolated and do not interact much with the B and Mo atoms. However, our calculations on the U needle within the $U_5Mo_{10}B_{24}$ complex indicate overlap populations on the order of those calculated for γ-U (0.35 in $U_5Mo_{10}B_{24}$ vs 0.29 in bulk U for uraniums 3.1 Å apart). In addition, there are short U−Mo contacts (3.0 Å) between collinear chains of U(3) and Mo(5). (The Mo atoms are displaced by 1.5 Å along the chain axis relative to the U atoms.) We see this interaction in Figure 5 in the Mo−U bonding and antibonding peaks around −9.5 and −4.5 eV, respectively. In addition to the direct spatial interactions between Mo and U, there is also a charge transfer from the $(Mo_{10}B_{24})^{20-}$ sublattice to the U_5^{20+} sublattice. Most of the electrons donated to the U sublattice are from Mo, which goes from a −9.5 to a +1.5 charge on 10 molybdenums. The molybdenum-based states that are depopulated are Mo−Mo antibonding, so the charge transfer from the interaction of the U sublattice with the molybdenum boride sublattice yields stronger Mo−Mo bonds than those in $(Mo_{10}B_{24})^{20-}$ as seen from the increased OP (see Table 1).

Conclusions

The B−B bonding in the isolated polyboride structures of $U_5Mo_{10}B_{24}$ is maximized with closed-shell electron counts of B_{14}^{16-}, B_{10}^{12-}, and B_7^{10-}. There is an interesting uncertainty in the possible electron counts for $^1_\infty[B_7]$ (**4**), which arises from questions of axial bonding at the central B in the column. Our calculations show that the additional electron in B_7^{11-} is found mostly on the outer edge of the polyacetylenic chains and not on the central B, and as a result it diminishes the π bonding in those polyacetylenic chains. So we feel that the geometry of **4** indicates a charge of 10− on $^1_\infty[B_7]$, **4**. Thus in each unit cell we have B_{48}^{60-}. The Mo−Mo cluster bonding is maximized for Mo^{1+} or Mo_{20}^{20+} per unit cell. This yields U_{10}^{20+}, two electrons per uranium. There does appear to be some U−U bonding, judging from the short (3.1 Å) contacts found in the lattice, so

the 4+ oxidation state on U rather than a possible 6+ seems reasonable.

There are a lot of close Mo−B contacts. Through these interactions the Mo's achieve a higher effective electron count of between 11 and 17 than they would have in the isolated clusters. These interactions (and subsequent electron transfer) lead to a loss of Mo−Mo bonding, but the gain in Mo−B bonding is great.

The stoichiometry of $U_5Mo_{10}B_{24}$ is unique and might appear to be related to a compound of formula UMo_2B_5. However, there is not precedent for a 1:2:5 stoichiometry of a rare-earth transition-metal boride.[24] In fact, when the compound was originally made it was tentatively assigned a 1:2:6 stoichiometry. $ThCr_2B_6$ ($CeCr_2B_6$ structure type) matches the intended stoichiometry and contains somewhat similar elements; one might wonder why $U_5Mo_{10}B_{24}$ crystallizes in such a complex structure (see Scheme 1) instead of the simpler (and related) $CeCr_2B_6$ structure type.

The electron counts of the rare-earth and transition-metal elements in $ThCr_2B_6$ and $U_5 Mo_{10}B_{24}$ are the same (4+ and 1+ (or d^4), respectively), despite the higher metal:boron ratio in $U_5Mo_{10}B_{24}$. It follows from the resulting higher negative charge per B atom that the polyboride structures in $U_5Mo_{10}B_{24}$ must have a lower connectivity. The lower connectivity of the boride substructures leaves larger channels in the crystal structure which allow more metal−metal contacts. The increased connectivity between Mo's would not be possible, or as desirable, for Cr in $ThCr_2B_6$, and this might explain why the $U_5Mo_{10}B_{24}$ structure (and stoichiometry) is observed instead of $U_5Mo_{10}B_{30}$.

Appendix 1: Electron Counting Around the Molybdenums

Let's first consider the B_6 coordination (from **3**) to Mo(1). The interaction is presumably between the π system of the ring and the corresponding orbitals on the molybdenum. For the middle two strips of fused rings there is a MoB_2 stoichiometry, because the borons in each ring also belong to three other rings. Thus there are only two electrons from the π system that can be donated to each Mo(1) from each ring. Using the same reasoning, the B_6 rings of **2** each have two π electrons to interact with each Mo(4). The edge B_6 rings of **3** have an MoB_3 stoichiometry, so there are three π electrons from each ring for each Mo(3).

The B_8 rings of **2** can be viewed as two fused B_5 rings, each coordinating an Mo(2). The B atoms at the "fold" of the kinked sheet carry a 2− charge (as described in the second section); the other B atoms have a formal 1− charge as with the graphitic B substructures. Because the latter B's are shared by 3 rings, these three borons can use one electron in total from their π system to interact with Mo(2). The bridging B's each have one

(22) Hoffmann, R. *Adv. Chem.* **1964**, *42*, 78.
(23) Alvarez, S. Unpublished results, 1993.
(24) Villars, P.; Calvert, L. *Pearson's Handbook of Crystallographic Data for Intermetallic Phases*, OH, 2nd, ed.; ASM International: Materials Park, 1991.
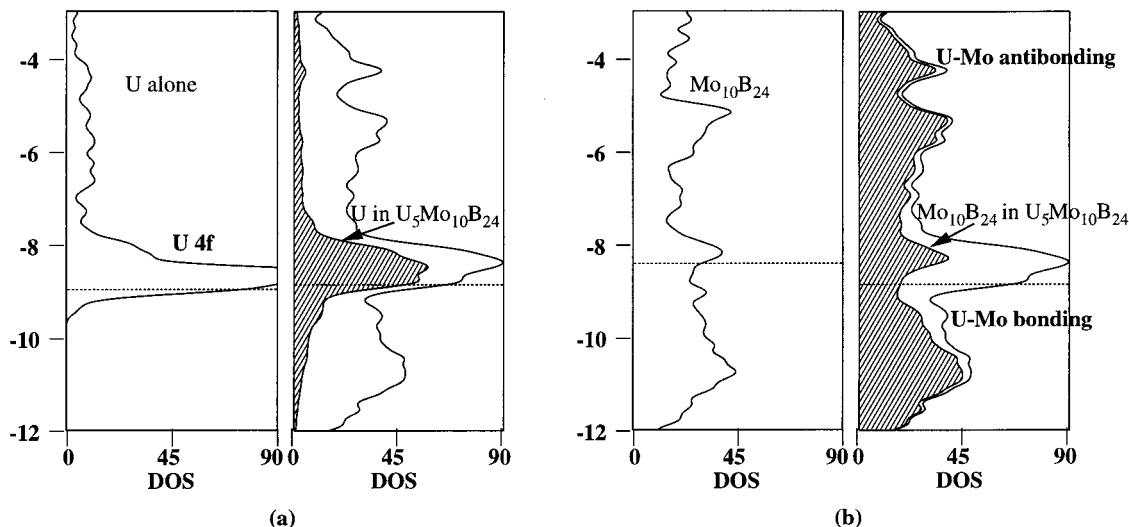
Figure 5. DOS plot of $U_5Mo_{10}B_{24}$ compared with the DOS plots for $(Mo_{10}B_{24})^{20-}$ and U_5^{20+} sublattices. (a) DOS of the isolated U sublattice (left) and contribution of U sublattice to $U_5Mo_{10}B_{24}$ (shaded at right). (b) DOS of $Mo_{10}B_{24}$ sublattice (left) and contribution of molybdenum boride sublattice to $U_5Mo_{10}B_{24}$ (shaded at right).

Table 2. Parameters Used in the Extended Hückel Calculations

atom	orbital	H_{ii}	ζ_1	$c_1{}^a$	ζ_2	$c_2{}^a$	ref[b]
B	2s	−15.20	1.30				22
	2p	−8.50	1.30				
Mo	5s	−8.50	3.50				23
	5p	−6.00	3.50				
	4d	−9.50	4.54	0.5814	2.00	0.5814	
U	7s	−3.50	3.50				23
	7p	−3.50	3.50				
	6d	−7.19	2.58	0.7608	1.21	0.4126	
	5f	−8.62	4.94	0.7844	2.11	0.3908	

[a] Coefficients in double-ζ expansion. [b] Mo and U parameters were modified from those in the given reference to eliminate problems with counter-intuitive orbital mixing.

electron in the π system of each B_5 ring, giving one π electron per ring. In total, there are two π electrons from the B_8 rings to bond with each Mo(2). Mo(6) is coordinated to a B_8 ring from **4** similar to that found in the kinked sheets. If we describe this as two fused B_5 rings coordinated to Mo(6), we have six π electrons for each Mo(6). (Recall that these rings are not part of a two-dimensional sheet, so the outer B atoms of the B_8 ring are not shared with other rings and can thus use all their π electrons in bonding to this molybdenum.)

The borons bridging the Mo(1)−Mo(2) and Mo(3)−Mo(3) bonds are from the polyacetylenic chains in **4**. The edges of the graphitic ribbons (**3**) are bridging the Mo(4)−Mo(5) bonds. In both of these cases there could be a donation to the Mo atoms from the "lone pair" on the outer edge borons. These sets of 2 edge borons and the corresponding two molybdenums are actually part of an extended chain, each lone pair is shared between two sets of molybdenums. The net contribution is two

electrons from these two borons, one to each Mo.

If we sum up the formal contributions of electrons to each Mo from B and add to that an electron from each Mo neighbor and the five d electrons originally on that Mo, we get formal effective electron counts around the molybdenums of 11 [Mo(1) and Mo(4)], 14 [Mo(2), Mo(3), and Mo(5)], and 17 [Mo(6)].

Appendix 2: Computational Details

The calculations presented in this work are in the framework of the extended Hückel[25−29] tight-binding method,[21,20,30] and used the YAeHMOP package[31] with f orbitals.[19] The off-diagonal elements of the Hamiltonian were evaluated with the modified Wolfsberg−Helmholtz formula.[32] Numerical integrations over the symmetry-unique section of the Brillouin zone of the one-dimensional structures were performed with a set of 100 k-points. The two-dimensional systems were calculated with 40 k-points, and the three-dimensional structure calculations used 48 k-points. The parameters used in our calculations are listed in Table 2.

(25) Hoffmann, R.; Lipscomb, W. N. *J. Chem. Phys.* **1962**, *36*, 2179.
(26) Hoffmann, R.; Lipscomb, W. N. *J. Chem. Phys.* **1962**, *36*, 3489.
(27) Hoffmann, R.; Lipscomb, W. N. *J. Chem. Phys.* **1963**, *37*, 520.
(28) Hoffmann, R. *J. Chem. Phys.* **1963**, *39*, 1397.
(29) Whangbo, M.-H.; Hoffmann, R. *J. Am. Chem. Soc.* **1978**, *100*, 6093.
(30) Whangbo, M.-H.; Hoffmann, R.; Woodward, R. B. *Proc. R. Soc. London, Ser. A* **1979**, *366*, 23.
(31) Landrum, G. A. The YAeHMOP package is freely available on the WWW at: http://overlap.chem.cornell.edu:8080/yaehmop.html.
(32) Ammeter, J. H.; Bürgi, H.-B.; Thibeault, J. C.; Hoffmann, R. *J. Am. Chem. Soc.* **1978**, *100*, 3686.